



# Simulating pathways of subsurface oil in the Faroe–Shetland Channel using an ocean general circulation model

C.E. Main<sup>a, b, c, \*</sup>, A. Yool<sup>a</sup>, N.P. Holliday<sup>a</sup>, E.E. Popova<sup>a</sup>, D.O.B. Jones<sup>a</sup>, H.A. Ruhl<sup>a</sup>

<sup>a</sup> National Oceanography Centre, European Way, Southampton SO14 3ZH, United Kingdom

<sup>b</sup> Ocean and Earth Science, University of Southampton, Waterfront Campus, European Way, Southampton, SO14 3ZH, United Kingdom

<sup>c</sup> Royal Society for the Protection of Birds, Western Isles Office, Seilebost, Harris, HS3 3HP, United Kingdom

## ARTICLE INFO

### Article history:

Received 25 March 2016

Received in revised form 16 September 2016

Accepted 19 September 2016

Available online xxx

### Keywords:

Oil spill

Blowout

Plumes

Pollution

GCM

## ABSTRACT

Little is known about the fate of subsurface hydrocarbon plumes from deep-sea oil well blowouts and their effects on processes and communities. As deepwater drilling expands in the Faroe–Shetland Channel (FSC), oil well blowouts are a possibility, and the unusual ocean circulation of this region presents challenges to understanding possible subsurface oil pathways in the event of a spill. Here, an ocean general circulation model was used with a particle tracking algorithm to assess temporal variability of the oil-plume distribution from a deep-sea oil well blowout in the FSC. The drift of particles was first tracked for one year following release. Then, ambient model temperatures were used to simulate temperature-mediated biodegradation, truncating the trajectories of particles accordingly. Release depth of the modeled subsurface plumes affected both their direction of transport and distance travelled from their release location, and there was considerable interannual variability in transport.

© 2016 Published by Elsevier Ltd.

## 1. Introduction

Modern societies remain largely dependent on crude oil as a material and energy resource. This has pushed the frontiers of oceanic oil drilling to exploit previously inaccessible reserves, for example those found on the continental slope. Deepwater drilling is expanding and programmes exist in various regions worldwide, for example, the USA, UK, Faroe Islands, New Zealand, Norway, Canada, Angola and Brazil (Leffer et al., 2011). The Faroe–Shetland Channel (FSC) has been undergoing development as an area for deepwater drilling for oil since the 1990s (Smallwood and Kirk, 2005). If a prolonged oil spill were to happen in the FSC, complex ocean currents in the region would present challenges to predicting or understanding the impacts of the contamination. Significantly, the FSC is an oceanic region that forms important habitat for a diverse array of benthic marine life (Bett, 2001; Jones et al., 2007). This is partly a result of the habitat heterogeneity in vertical and horizontal temperature gradients that are caused by the influence of cold Arctic bottom water underlying warmer currents at the surface. Several large areas of the FSC have been designated as marine protected areas, for example the North-east Faroe–Shetland Channel (Joint Nature Conservation Committee, a) and Faroe–Shetland Sponge Belt Nature Conservation Marine Protected Areas (Joint Nature Conservation Committee, b).

The 2010 Macondo oil well blowout was the largest accidental release of hydrocarbons into the deep sea from a single incident, with estimates for the total amount of oil spilled reaching 4.9 million barrels (approximately  $7.8 \times 10^8$  L, McNutt et al., 2011) over the prolonged (86 days) release of crude oil and gas into the deep (~1600 m) waters of the Gulf of Mexico (GoM). Following the incident, there was uncertainty in the true amount of oil spilled, where it went and what effects it had on biota in the deep sea. This was because it became clear that a large proportion of the oil, perhaps > 30% of the total amount released (Ryerson et al., 2012; Reddy et al., 2011) never reached the surface, and uncertainties in the oil droplet size distribution complicate the estimation of the amount of subsurface oil (Ryerson et al., 2012). Various mechanisms resulted in oil from plumes of dissolved oil and small droplets reaching the seabed over a wide area, and although some of the impacts of this oil on the resident benthos have been documented (White et al., 2012) the true areal extent of the spilled oil's benthic distribution and effects remain uncertain (Montagna et al., 2013), though is likely to have been considerable (Valentine et al., 2014).

The progression of crude oil leaking from an oil well blowout and the subsequent pathways it takes in the subsurface ocean depends on its buoyancy. This buoyancy in turn depends on the proportion of gas emitted, subsequent gas hydrate formation, and oil droplet size and composition (Johansen, 2003; Yapa et al., 2008; Dasanayaka and Yapa, 2009). Biological and chemical weathering processes change oil composition in the environment and this also has an important effect on its behaviour in seawater. Many of the processes involved in weathering are highly temperature dependent. Oil from the Macondo well blowout flowed as a hot (~100 °C), high pressure jet into the

\* Corresponding author at: National Oceanography Centre, European Way, Southampton, SO14 3ZH, United Kingdom.

Email address: charlottemain@gmail.com (C.E. Main)

much cooler ( $\sim 4\text{ }^{\circ}\text{C}$ ) surrounding ocean (Reddy et al., 2011). As the main column of oil, gas and droplets was propelled rapidly towards the surface, small ( $< 100\text{ }\mu\text{m}$  diameter) droplets of oil were able to form a neutrally buoyant layer of hydrocarbons that remained at between 800 and 1300 m water depth, as predicted by Socolofsky et al. (2011) and observed by Camilli et al. (2010). The use of chemical dispersants at the Macondo wellhead further encouraged the formation of small oil droplets (National Research Council, 2005) and was likely to have suppressed biodegradation by microorganisms (Kleindienst et al., 2015). Some lighter molecular weight compounds, including natural gas and monoaromatic hydrocarbons: benzene, toluene, ethyl-benzene and xylene (collectively: BTEX) dissolved in the seawater, contributing to the formation of large, neutrally buoyant, subsurface plumes of dissolved hydrocarbons and droplets. Such plumes provide a route by which spilled oil can be transported on ocean basin scales, with fallout from the plumes potentially contaminating vast areas of the deep ocean, as was observed in the GoM (Valentine et al., 2014).

The GoM plumes triggered blooms of indigenous deep-sea bacteria including  $\gamma$ -Proteobacteria, a group that are related to petroleum degraders (Hazen et al., 2010). The response of deepwater bacterial communities was strong enough to cause appreciable local oxygen anomalies as they respired dissolved methane (Kessler et al., 2011), propane and ethane (Valentine et al., 2010). Temperatures of  $\sim 4\text{ }^{\circ}\text{C}$  in the deep GoM appeared to favour certain genera of bacteria (*Oceanospirillales*, *Cohwelia* and *Cycloclasticus*) that were found at depth but not in surface slicks of oil (Redmond and Valentine, 2011).

Circulation models helped to advance the understanding of the fate of hydrocarbons following the Macondo spill (Adcroft et al., 2010; Liu et al., 2011a; Mariano et al., 2011; Valentine et al., 2012; Paris et al., 2012; Lindo-Atichati et al., 2014). Ocean circulation models were utilised operationally to simulate the oil's transport, both at and below the surface (Liu et al., 2011b; Mariano et al., 2011). Circulation models were also used to study the potential extent of deep plumes of hydrocarbons following the Macondo spill (Adcroft et al., 2010; Paris et al., 2013; Lindo-Atichati et al., 2014), and to model their effects on resident pelagic microbial communities (Valentine et al., 2012).

As the above outlines, what has been learned about the fate and effects of spilled oil in the deep sea has been concerned largely with the oceanic conditions present in the GoM at the time of the Macondo spill. However, oil drilling is continuing to increase in areas outside the GoM, for example the FSC, where to date there have not been accidental oil well blowouts. Little is known about the potential fate and effects of accidental deepwater releases of oil in this oceanographically contrasting region, although an experiment involving the release of oil at the seabed in 844 m at a site in the Norwegian Sea has provided some data with which to validate models (Johansen et al., 2003).

A particular consideration in the FSC region lies with its circulation. The seabed topography of the Greenland-Scotland ridge gives rise to a complex exchange of water between Nordic seas and the north Atlantic and this presents challenges to the prediction of pathways of subsurface oil in the region. At, and near the surface, water of the North Atlantic Current passes from the Atlantic northwards towards the Arctic in the two branches of the Norwegian Atlantic Current (NwAC, Rossby et al., 2009). The other main near-surface current in the FSC is formed from Modified North Atlantic Water (MNAW), which dominates surface waters of the FSC in areal extent. This current originates from the Atlantic but enters the FSC from northeast of the Faroe Islands. It is then re-circulated to join the NwAC flowing into the Norwegian Sea (Turrell et al., 1999). Hence, very little surface water leaves the FSC to the south.

At depth, however, the circulation is largely in the opposite direction to the surface currents. The warm surface waters of the NwAC cool and lose buoyancy as they progress northwards to the Arctic. These sinking waters form a large proportion of the deep water formed in this region. Subsequently, bottom water formed in the Nordic Seas flows southwards at depth, and FSC Bottom Water is a mix of intermediate water and deep water from the Nordic Seas (mainly Norwegian Sea Arctic Intermediate Water and Norwegian Sea Deep Water). The Wyville Thomson Ridge (WTR), with a sill depth of  $\sim 450\text{ m}$ , presents a barrier to southward flow of the cold water mass of the deep FSC. Hence, although bottom water occasionally cascades over the WTR (Sherwin and Turrell, 2005), around  $2.7 \pm 0.5\text{ Sv}$  flows westward over a sill at  $\sim 850\text{ m}$  to enter the Faroe Bank Channel (FBC, Berx et al., 2013).

Three-dimensional ocean general circulation models (GCMs) have been developed to study ocean currents and patterns in transport on regional and global scales. Forced at the surface boundary with atmospheric reanalysis data (Dussin and Barnier, 2013), they provide detailed and realistic representations of the ocean state (Madec, 2008). Through comparison with field observations and exploration of physical processes, GCMs have enhanced our understanding of thermohaline circulation (Lohmann et al., 2014), transport pathways (Blanke et al., 1999) and bulk properties over ocean-basin scales (Marzocchi et al., 2015). However, full simulations of ocean physics and biogeochemistry using GCMs are expensive in terms of both raw computational cost and output storage requirements, especially at high resolution. One alternative approach, particularly in the context of studying transport, is to use Lagrangian particle-tracking algorithms (PTA). These provide a means of studying pathways using existing modelled circulation at a fraction of the cost of the full GCM. Lagrangian PTA releases of passive drifting 'particles' can be applied to study the passage of the currents themselves (Blanke et al., 1999), or indeed anything that can be considered a passive tracer of current flow, such as particulates (Jutzeler et al., 2014) or even small animals (Putman et al., 2012).

Here, output from a 3D GCM is used in conjunction with the 'Ariane' PTA (Blanke and Raynaud, 1997) to model the pathways of subsurface oil plumes emanating from simulated blowouts in the FSC. This study aims to understand the implications of an oil well blowout in the FSC by:

- 1) Investigating circulation pathways of oil at depths throughout the water column
- 2) Investigating inter- and intra-annual patterns in circulation pathways, and hence:
- 3) Highlighting key geographical areas of impact from fallout of contaminated material from near-seabed plumes.

## 2. Methods

### 2.1. The NEMO model

The Nucleus of European Modelling of the Oceans (NEMO) is a 'state-of-the-art' modelling framework for simulating ocean dynamics, sea-ice and ocean biogeochemistry (see: <http://www.nemo-ocean.eu/>). The model is composed of an ocean general circulation model, OPA (Madec, 2008), coupled with the Louvain-la-Nouve Ice Model v2, LIM2 (Timmermann et al., 2005). The version of NEMO used here is v3.5 and is configured at global scale with a horizontal resolution of  $1/12^{\circ}$  (eddy-resolving), with 75 levels in the vertical increasing from 1 m thickness at the surface to  $\sim 200\text{ m}$  at abyssal depths. The model ocean is forced at the surface by DFS reanalysis products developed as part of the European DRAKKAR collaboration, where

1994–2007 uses DFS 4.1 (Brodeau et al., 2010), and 2008 onwards uses DFS 5.1 (Dussin and Barnier, 2013). The full model was simulated from 1994 to 2009, and output, including velocity fields, stored as 5-day averages for this period.

The simulation used here has been extensively described and validated for the North Atlantic, sub-polar region by Marzocchi et al. (2015), who calculated volume transport in the model across five sections marking boundaries to the sub-polar North Atlantic domain, and extracted modelled sea surface temperature (SST) and sea surface salinity (SSS) to compare to UK Met Office datasets. Marzocchi et al. (2015) assessed the realism of large scale surface current patterns by comparing model output with geostrophic velocities derived from satellite altimetry. Modelled volume transport for Nordic Seas overflows (Denmark Strait overflow and Faroe Bank Channel overflow) was also extracted and compared to observational Eulerian datasets. The Marzocchi et al. (2015) study found that the 1/12° resolution model represented various oceanographic features more realistically than previous versions (1° and 1/4°), including – of particular relevance here – the position of the north Atlantic current and the transport of flows at the Greenland-Scotland ridge. Further validation exercises relevant to the study area here are presented in Supplementary Info.

## 2.2. Experiment design

A series of simulations were run to examine the role of both the timing and depth of oil release on its subsequent dispersal. Neutrally buoyant, dimensionless ‘particles’ were released and used to track subsurface trajectories of dissolved and small droplets of oil. Using the Ariane Lagrangian PTA, these passive particles, were released on a regularly spaced grid spanning approximately 0.5° latitude by 0.5° longitude at a location that has recently been drilled for oil in the FSC (Lagavulin well: 1567 m depth, 62.66° N, 1.126° W). Grids of 20 × 20 (= 400) particles were released at depth intervals spanning the water column from just below the surface (10 m), 50 m and then at 50 m intervals down to 1500 m. The dynamics of plume formation is complex and was not considered here. Particles were seeded into a horizontal area spanning ~ 55 km for each release. Releases of 400 particles × 31 depths (= 12,400 particles per “spill”) were supplied to Ariane once every month from January 1994 (allowing a 15 year period for model spin up) until December 2009, and allowed to drift for 365 days. The positions of released particles were recorded by Ariane at 5 day intervals, ultimately forming an output dataset spanning 16 years of releases. The final particle release date was December 2009, and Ariane simulations continued to December 2010 to permit this final release to drift for a full year. Hence, there were 12 releases per year for a total of 16 years, resulting in 192 releases of 12,400 particles, and therefore 2,380,800 particles in total.

As with other biogenic substances, oil is subject to biological breakdown. Hydrocarbon-degrading bacteria possess the enzymes necessary to be able to degrade oil, using it as a source of organic carbon and energy. Like other biological processes, this breakdown is strongly influenced by ambient temperature, with higher temperatures typically accelerating the rate of oil degradation. To factor this into our analysis, a simple decay-rate Eq. (1) was employed to decay particles at a rate (R) in relation to ambient temperatures and thus elucidate the importance of temperature controlled decay to limit oil spread. This simulated temperature-dependent biological weathering of oil, allowing an examination of how the distribution of oil may be impacted by ambient conditions encountered along trajectory tracks. Decay of particles was effected by using Eq. (1) to proportionately remove from particles at each step of the output in the simulation, un-

til a threshold was reached at which to terminate the particle's progression. An arbitrary threshold of 10% of starting value was set at which to terminate particle trajectories. The change in spread of oil was studied for this threshold in relation to the initial, undecayed results.

$$R^{-1} = 12 * 3^{-(T-20)/10} \quad (1)$$

Where T = ambient temperature.

To study the pathways along particular channels around the FSC, “traps” of 1.5° latitude × 1.5° longitude were defined and set at the main circulation pathways (Table 1). Any particle that arrived at one of these traps was counted (once) and these particles were then summed at respective times and depths of release to create an array of ‘hits’ for each trap location, for which standard deviation, median and interquartile range were calculated. The traps were used to assess advection of oil, and the importance of seasonal and interannual influences of its circulation pathways. The traps were not intended to catch all of the particles released, but instead to highlight spatial and temporal patterns of advection to particular regions.

Finally, contact with seafloor was calculated as the number of particle days that were within 200 m of the seafloor. Evidence suggests that near (300 m above) seafloor oil plumes from the leaking Macondo well in 2010 resulted in large areas (> 3200 km<sup>2</sup>) where a footprint of contamination formed (Valentine et al., 2014). The threshold depth of 200 m was chosen here as that at which contamination might reasonably be assumed to result from plume fallout at that geographical location.

## 3. Results

### 3.1. Advective pathways of spilled oil

Results will initially be described for particles that were allowed to drift for one year with no decay. Then the effect of simulated biological decay on trajectories is described. Pathways of particle trajectories from releases in the FSC were strongly determined by release depth (Fig. 1a-c). Particles released at depths of 200 m or shallower tended to be transported northwards from the release location into offshore and coastal branches of the NwAC (Fig. 1a). In some cases, these particles were then carried north to the Arctic towards Svalbard and into the Barents Sea. A further branch split off towards eastern Greenland to move again southwards close to the Greenland coast.

Particles released at intermediate depths 250–550 m also followed these pathways in many cases (Fig. 1b). However, these deeper releases resulted also in particles being carried west through the FBC and on to the Iceland basin. Other particles entered the North Atlantic

**Table 1**  
Traps locations.

Trap	Location	Coordinates
W1	Southeast Greenland	58.5–60.0°N; 43.5–42.0°W
W2	Iceland Basin	62.75–64.25°N; 15.25–13.75°W
W3	Wyville Thomson Ridge	59.25–60.75°N; 10.25–8.75°W
W4	Faroe Bank Channel sill	60.25–61.75°N; 8.5–7.0°W
W5	Faroe Shetland Channel	60.0–61.5°N; 5.5–4.0°W
E1	Norwegian Sea east	65.5–67.0°N; 5.0–6.5°E
E2	Norwegian Sea west	67.75–69.25°N; 2.5–4.0°E
E3	Sub-Arctic	68.5–70.0°N; 12.5–14.0°E
E4	Svalbard	78.0–79.5°N; 8.0–9.5°E
E5	Russian Arctic	71.5–73.0°N; 21.0–22.5°E

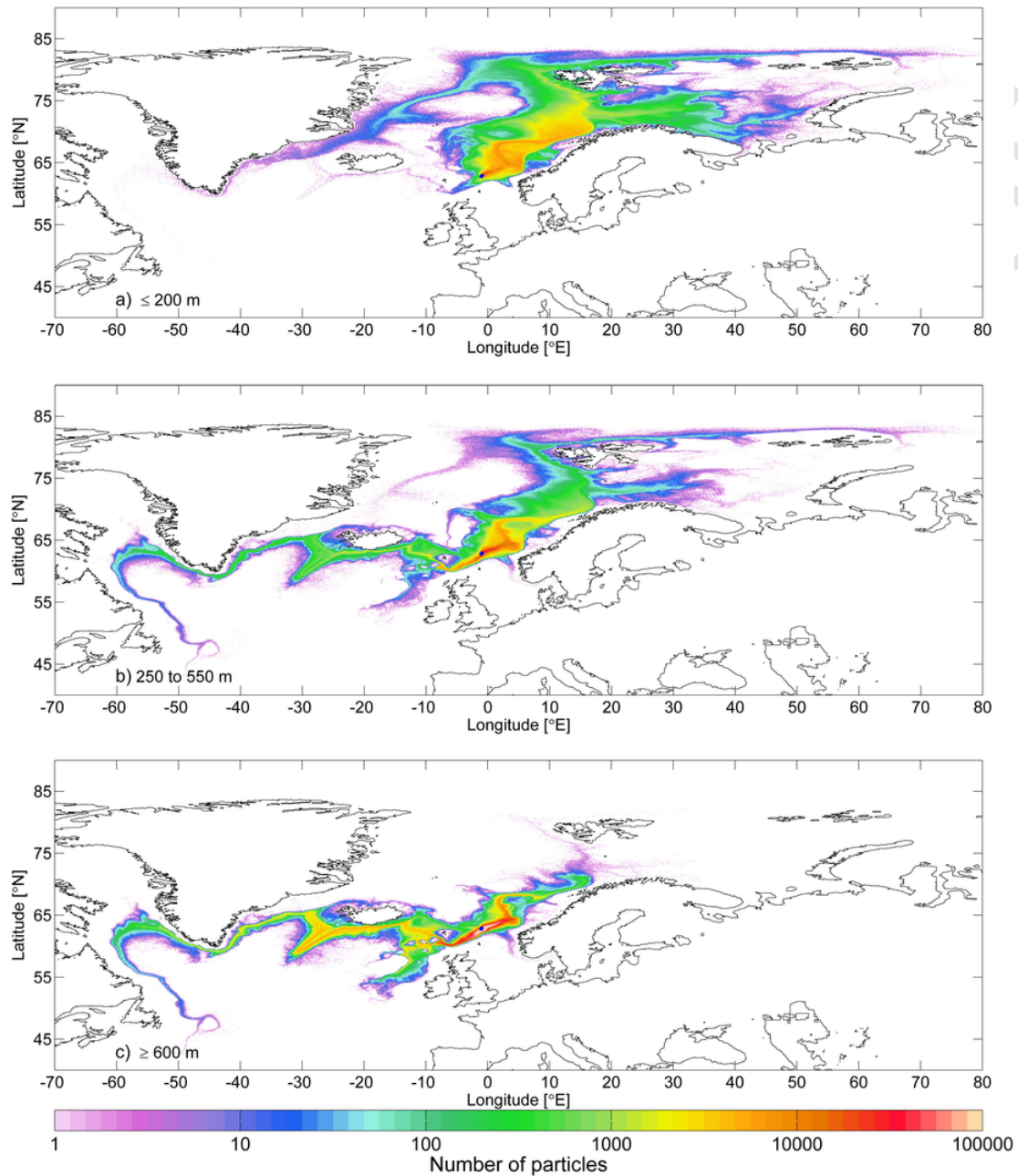


**Fig. 1.** Particle density plot representing all particles released each month between 1994 and 2009 and allowed to drift undecayed for 365 days from release depths of: a)  $\leq 200$  m; b) 250–550 m, and c)  $\geq 600$  m. Particle release locations are shown at  $62.66^\circ$  N;  $1.126^\circ$  W. Particle density is plotted on a logarithmic scale.

in a southward-directed flow through the Rockall Trough (Fig. 1b). Particles from these intermediate-depth releases that travelled west beyond the mid-Atlantic ridge appeared to be channelled southwards, traversing the ridge at the Charlie Gibbs Fracture Zone (Fig. 1b).

Particles released in the deepest water of the FSC ( $> 600$  m) did not generally progress as far north as the shallow particles and were instead more likely to flow west to be channelled over the sill through the FBC (Fig. 1c). Particles from deeper releases were able to reach as far west as southern Greenland, the Labrador Sea and on towards Newfoundland and the Grand Banks (Fig. 1b and c). A small number of particles from releases deeper than 250 m were advected around the southern Norwegian coast to enter the Skagerrak (Fig. 1b and c).

### 3.2. Transport to particular ocean areas

When summed across the 16 year period for each release, these cumulative particle densities indicated that, over time, transport to some ocean areas was much more intense than to others, according to circulation patterns in the model (Fig. 2). Fig. 2 indicates the composite density of particles released from all depths for the entire period studied, as well as the series of “traps” (Table 1) used to quantify particle transport along particular currents.

Release depth had a strong effect on particle counts at the traps (Table 2; Figs. 3 to 6). Traps located to the west of the release location (W1–W5) received particles from  $< 20\%$  of all shallow ( $< 200$  m) releases. In contrast, the eastern group of traps (E1–E5) re-

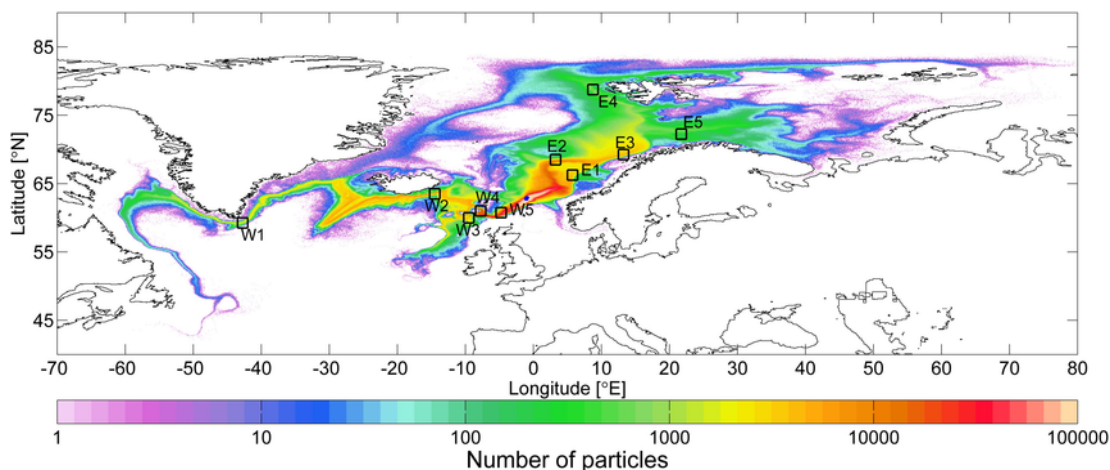


**Fig. 2.** Traps used in the analysis, shown superimposed over a particle density plot of particle locations following undecayed drift for 365 days of all particle releases 1994–2009. Particle depths are not shown. Particle release locations are shown at 62.66° N; 1.126° W. Particle density is plotted on a logarithmic scale.

**Table 2**

Percentage of all releases (1994–2009) from each release depth resulting in contamination (presence of any particles) at traps. Note that, because some particles never reach any traps, while others reach multiple traps, neither rows nor columns sum to 100%. Values  $\geq 50\%$  have been shaded.

Trap	W1	W2	W3	W4	W5	E1	E2	E3	E4	E5
Release depth (m)										
10	13				4	93	99	100	100	99
50	5			1	7	79	100	99	99	98
100	5	1	1	2	6	76	100	100	99	95
150		1	1	2	8	79	100	100	99	89
200	2	8	6	13	21	88	100	100	99	88
250	9	28	23	38	52	97	100	100	96	75
300	26	56	55	70	77	100	100	100	84	50
350	48	78	73	88	93	99	100	99	69	32
400	67	89	84	94	95	98	100	96	48	26
450	75	95	89	96	97	96	100	91	32	18
500	83	97	93	98	100	90	99	80	14	9
550	85	97	93	99	99	84	97	71	8	9
600	85	96	94	97	99	80	94	69	7	3
650	84	96	96	97	98	73	89	56	2	5
700	88	96	96	96	96	69	80	52	2	4
750	85	96	96	97	97	57	73	39	2	2
800	87	95	96	96	96	51	68	33	1	2
850	85	94	95	94	95	41	58	23		2
900	82	92	94	94	94	28	58	24	1	2
950	79	92	94	94	94	37	49	22		
1000	78	92	93	93	94	26	47	19		2
1050	72	91	93	92	93	32	41	14	1	
1100	65	91	92	92	93	20	40	17		1
1150	60	88	91	91	92	21	36	13	1	2
1200	57	85	90	90	90	22	30	8		1
1250	51	80	84	85	87	24	29	12	1	
1300	52	76	81	81	84	15	27	8	1	1
1350	46	75	77	80	81	19	20	8	1	1
1400	44	73	76	76	79	21	19	10	2	1
1450	46	70	74	75	78	18	17	7	1	2
1500	45	69	73	76	77	18	16	8	1	1

ceived particles from 75 to 100% of the releases from these shallow depths (Table 2).

Trap W5, which was positioned at the FSC close to the release location received the highest proportion of particles overall. Particle capture at this trap indicated that downstream transport of oil plumes remaining at depth was mainly to the west, with  $> 50\%$  of all particles released at depths  $> 250$  m reaching the trap.

Also in the FSC study-area, trap (W3) was located over the WTR. Particles flowing west from deep water releases ( $> 600$  m) were seen to periodically cascade over the sill at the WTR (Fig. 4, W3). As expected though, most of the westward flow was channelled over the FBC sill (trap W4, Fig. 4) and into the FBC.

The results also highlighted interannual variability in flow, and several periods of strong winter flow. As shown in Fig. 4, high proportions ( $> 90\%$  of each release from 500 to 1000 m depth) of the particles reaching the FSC, W5 trap were caught in prolonged periods between late 2000 and 2002. There was a further period of prolonged high capture-rate in late 2007 to early 2009. A lower proportion ( $< 80\%$ ) of released particles reached the trap during 2005 to 2007. Trap W2 (Iceland basin) caught almost no particles from any release during 1994. However, from 1995 onwards, this trap received particles (20–50% of those released) from most intermediate depth (600–1000 m) releases (Fig. 3). At Southwest Greenland higher ( $> 20\%$ ) particle counts at trap W1 tended to occur in winter (11 of the 16 years studied).

Particles reaching the Norwegian Sea (traps E1 and E2) were consistently those released from depths shallower than 400 m. This occurred year-round throughout the time series of releases, but with occasional gaps (Fig. 5). Particles were generally transported in greater numbers to offshore regions of the Norwegian Sea (trap E2), but with two periods (1996–2000 and 2003–2005) where the more inshore areas of the Norwegian Sea (trap E1) received more, suggestive of a switch in the main flow pathways during these periods. Although particles from shallow releases dominated eastward transport, the offshore trap (E2) also sporadically received particles from releases spanning the water column (e.g. in 1994 and 2005).

Particles travelling towards the sub-Arctic were caught by trap E3, with winter releases clearly resulting in higher proportions ( $> 70\%$ ) of particles reaching the trap (Fig. 6, E3). Traps E4 and E5 were located in the Arctic, and received relatively low proportions of particles ( $< 10\%$ ) from many of the shallow water ( $< 300$  m) releases (Fig. 6). Interannual variability and strong winter flow was again evident, with winter releases resulting in higher proportions of particles reaching the Arctic (up to 50% of releases in the winters of 2002 and 2005, for example).

When particle decay was considered, the horizontal spread of particles was significantly reduced (Fig. 7) and the average decay time (to 10%) did not exceed 250 days. Particles terminated on reaching 10% of their initial value were not transported nearly as far in most

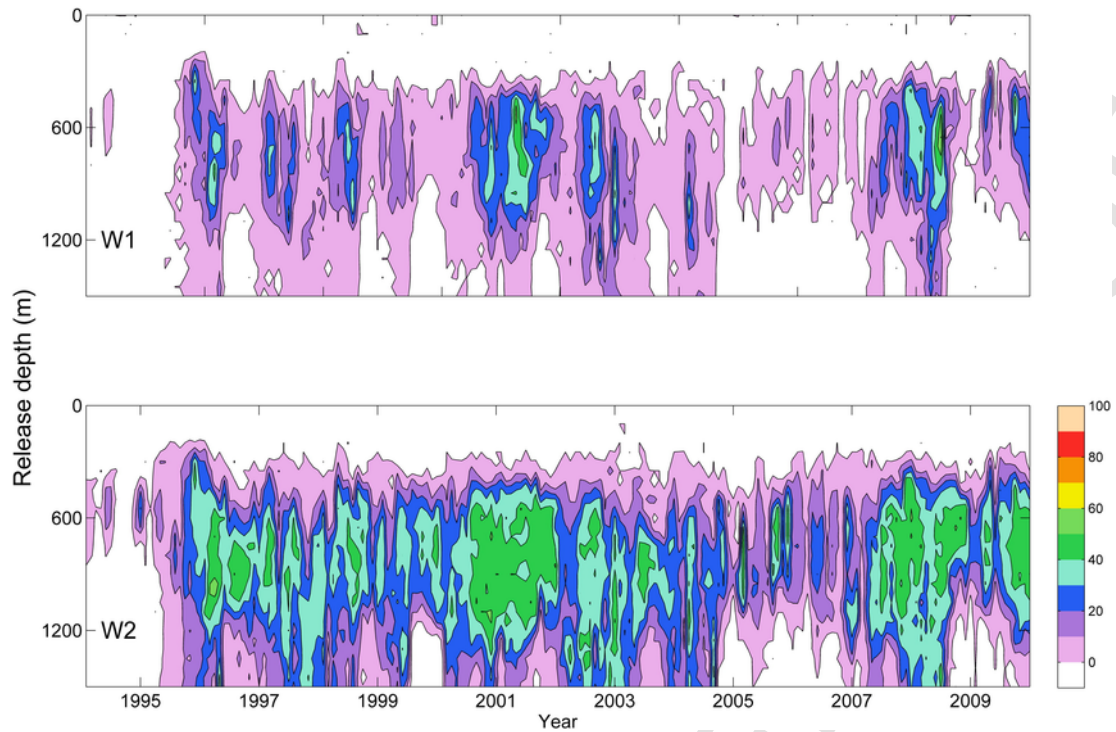


**Fig. 3.** Percentage of particles from each undecayed release reaching traps, plotted by release time (horizontal axis) and release depth (vertical axis). W1: Southeast Greenland; W2: Iceland basin. See text for explanation of traps and their locations.

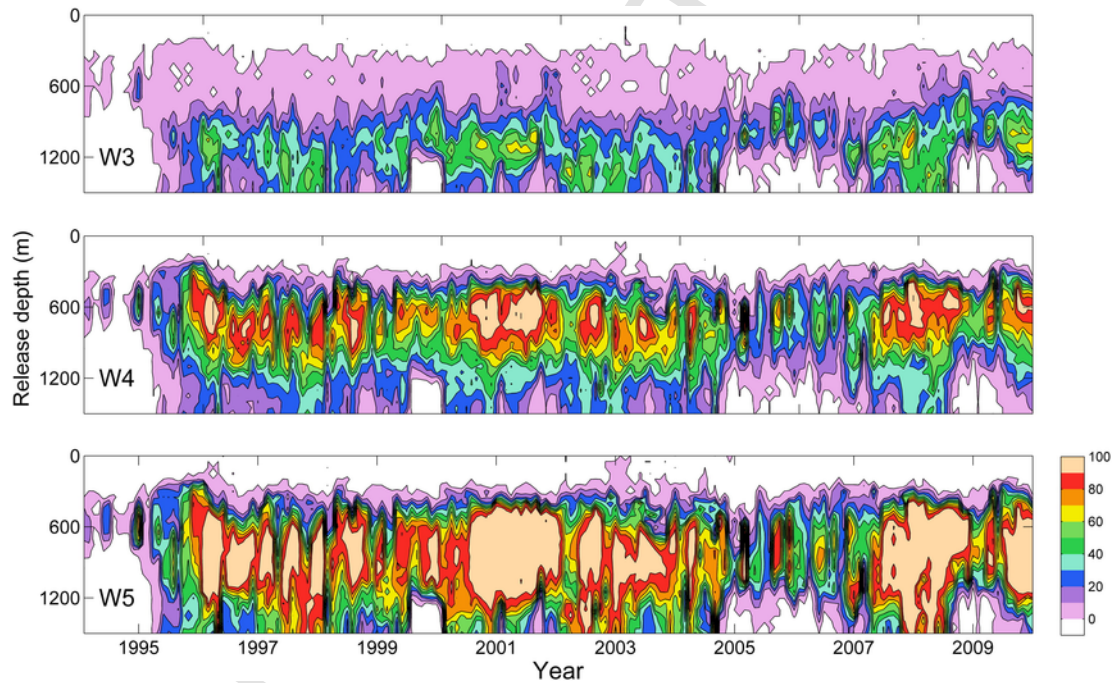


**Fig. 4.** Percentage of particles from each undecayed release reaching traps, plotted by release time (horizontal axis) and release depth (vertical axis). W3: Wyville Thomson Ridge; W4: Faroe Bank Channel; W5: Faroe Shetland Channel. See text for explanation of traps and their locations.

cases, and some traps received few (E4, E5) or no particles (W1) from any release once the potential for decay was considered (Fig. 7; Table 3). As would be expected given the temperature dependence of the decay function, particles released in shallower, warmer seawater experienced faster decay than those released in deeper, colder waters,

meaning that the effect of decay was highly apparent at particle traps located furthest to the north (Fig. 7) where only small proportions (< 5%) of shallow (200–350 m) releases resulted in capture in the Arctic traps E4 and E5 (Fig. 7; Table 3).

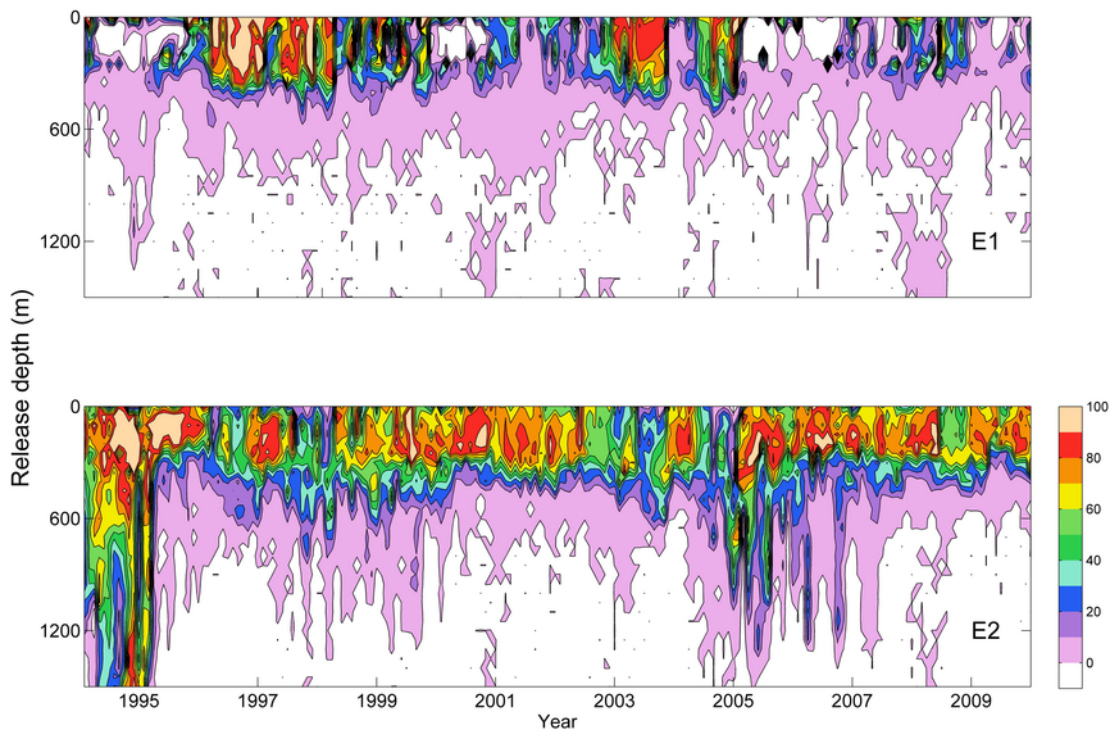


**Fig. 5.** Percentage of particles from each undecayed release reaching traps, plotted by release time (horizontal axis) and release depth (vertical axis). E1: Norwegian Sea east; E2: Norwegian Sea west. See text for explanation of traps and their locations.

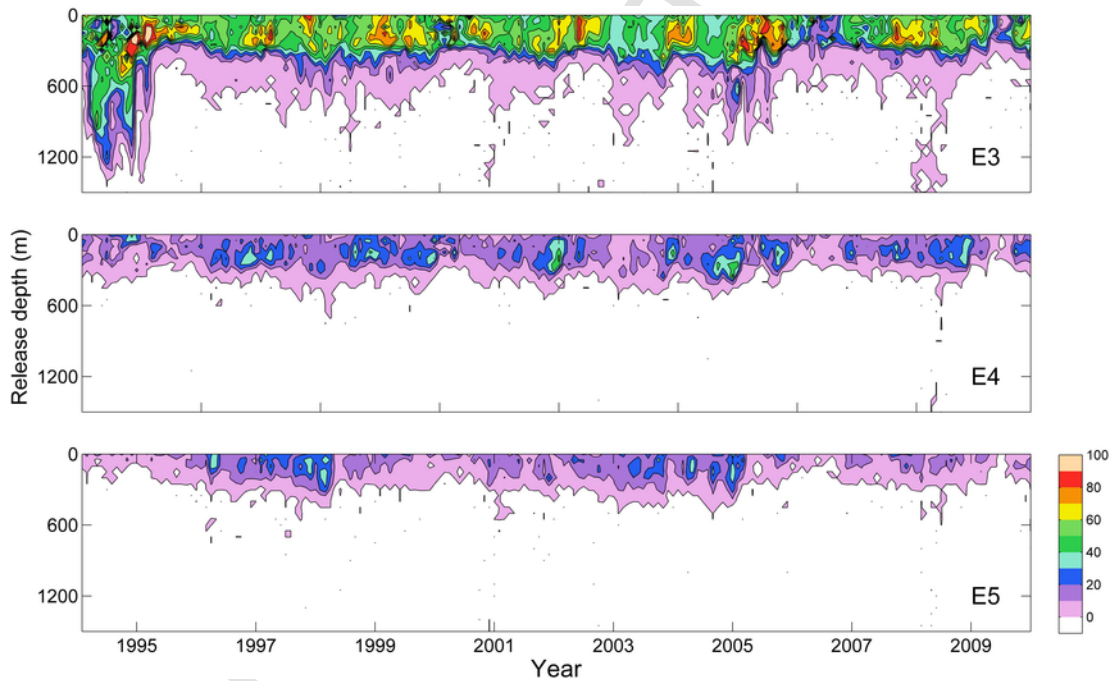


**Fig. 6.** Percentage of particles from each release reaching traps, plotted by release time (horizontal axis) and release depth (vertical axis). E3: Sub Arctic; E4: Svalbard. E5: Russian Arctic. See text for explanation of traps and their locations.

**3.3. Geographical areas of seafloor impact**

Release depth also affected the location and extent of the geographical areas of the seabed that were contaminated by particles

(Fig. 8). Particles released in < 450 m water depth mainly contacted the seabed along the shelf edge break of the FSC and Norwegian Sea and reached the Barents Sea and the Arctic around Svalbard (Fig. 8a). Although most of the transport was to the east, some shallow releases

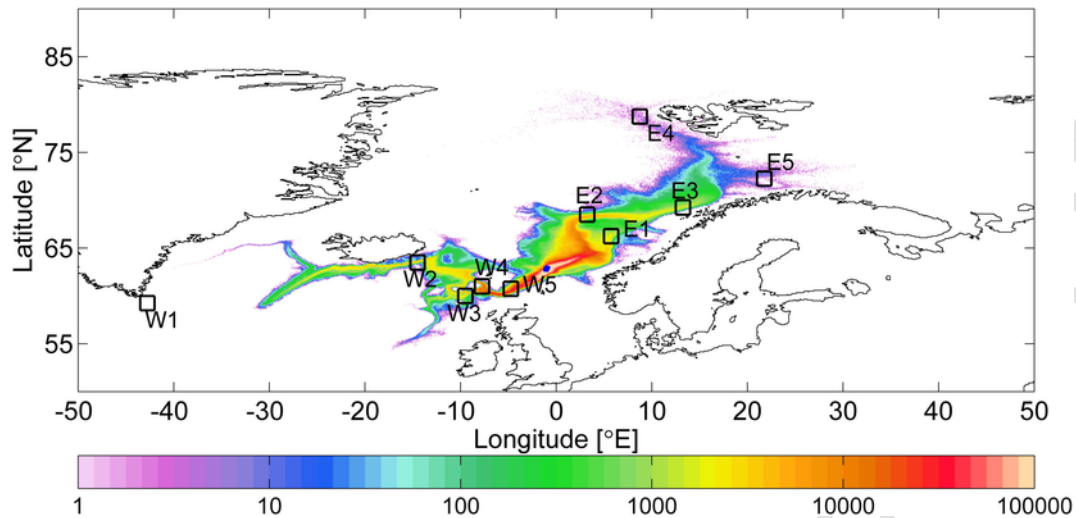


**Fig. 7.** Particle density plot of decayed particle positions following termination of their drift on reaching 10% of their initial size with trap locations superimposed. Plot shows particle positions following all releases 1994–2009. Particle depths are not shown. Particle release locations are shown at 62.66° N; 1.126° W. Particle density is plotted on a logarithmic scale.

**Table 3**

Percentage of all releases (1994–2009) resulting in contamination (presence of any particles) at traps following decay to 10%. No particles reached trap W1 under this condition. Values > 50% have been shaded.

	W1	W2	W3	W4	W5	E1	E2	E3	E4	E5
Release depth (m)										
10					1	83	83	78	9	15
50					1	71	89	83	6	16
100						66	92	94	5	12
150				1	1	70	96	93	3	5
200		1		2	3	74	95	90	1	4
250		6	7	9	16	89	94	79	2	3
300		18	15	30	42	90	95	65	1	2
350		35	31	52	60	77	90	44	1	2
400		56	49	76	81	57	85	26		
450		70	57	83	87	40	72	18		
500		80	61	87	90	26	55	10		
550		83	61	89	91	15	44	6		
600		86	73	89	91	7	39	5		
650		86	81	90	91	4	30	4		
700		89	87	91	91	2	24	4		
750		89	91	91	91	2	24	3		
800		86	90	91	92	1	22	3		
850		85	90	91	92		19	3		
900		83	89	89	91	1	16	3		
950		81	90	90	91	2	16	3		
1000		75	88	90	90	1	16	2		
1050		72	88	89	90	1	16	2		
1100		68	84	85	89		13	1		
1150		62	78	81	84		11	1		
1200		57	75	77	82		8	1		
1250		54	69	70	76		7	1		
1300		52	65	67	73	1	6	1		
1350		48	63	63	70		5			
1400		47	61	63	69		4			
1450		45	61	61	69		4			
1500		48	61	63	67		4			

of particles were transported west across the Greenland-Scotland ridge in overflow water.

Particles released at intermediate depths (500–950 m) were mainly transported west, and areas of the FSC, FBC, Iceland basin, mid-Atlantic ridge and beyond were instead impacted (Fig. 8 b). Particles released in deep water close to the seafloor (1000–1500 m)

were slightly more confined to the FSC (in slower deepwater currents) but also reached the Iceland basin and mid-Atlantic ridge. (Fig. 8c). Particle decay limited the average area of seafloor contact considerably (Fig. 9). However, the impact of deep releases still reached as far as the mid-Atlantic ridge and a small number of shallow-released particles (< 1%) still reached the Arctic (Fig. 9). There was interannual variability in the average number of particle days from each release that were within 200 m of the seafloor (Table 4), with somewhat lower proportions of particle days contacting the seafloor in 2005 and 2006, except for the deepest releases. Figs. 4 and 5 also indicated that there was more transport to the north (Norwegian Sea and beyond) in the NwAC and other currents in these two years.

#### 4. Discussion

In the simulations, release depth had a strong directional effect on particle spread, and also on the extent of their travel, when considering both undecayed and decayed releases. Near to the surface (< 300 m depth) most of the released particles were advected northwards in the model's two branches of the relatively warm (~ 10 °C average) NwAC. Deeper (> 600 m) releases were more likely to be advected to the west in cold (< 0 °C) bottom water, with most of the flow travelling over the Greenland-Scotland ridge at the FBC sill. These results reflect previous observations of the circulation in the region, thus indicating that the model is an effective indicator of the pathways of dissolved and neutrally buoyant oil resulting from a deep water oil well blowout in the FSC. Long term oceanographic measurements in the FSC have shown that bottom water formed in the Arctic must traverse the Greenland-Scotland ridge in order to enter the north Atlantic (Turrell et al., 1999; Sherwin et al., 2006). While much of this crosses the sill at ~ 850 m depth into the FBC, occasional cascades over the Wyville Thomson Ridge are caused by internal waves (Sherwin and Turrell, 2005). Well-studied surface currents in the region of interest include the NwAC, which has a strong flow ( $5.1 \pm 0.3$  Sv) that separates into two main branches, the strongest of which ( $3.4 \pm 0.3$  Sv) is the inshore, eastern branch (Mork and Skagseth, 2010). In agreement with these observations, the modelling results also showed that shallow (< 300 m depth) releases of particles flowed in two main branches to traverse the Norwegian Sea. These shallow releases were most likely to be carried furthest from their re-

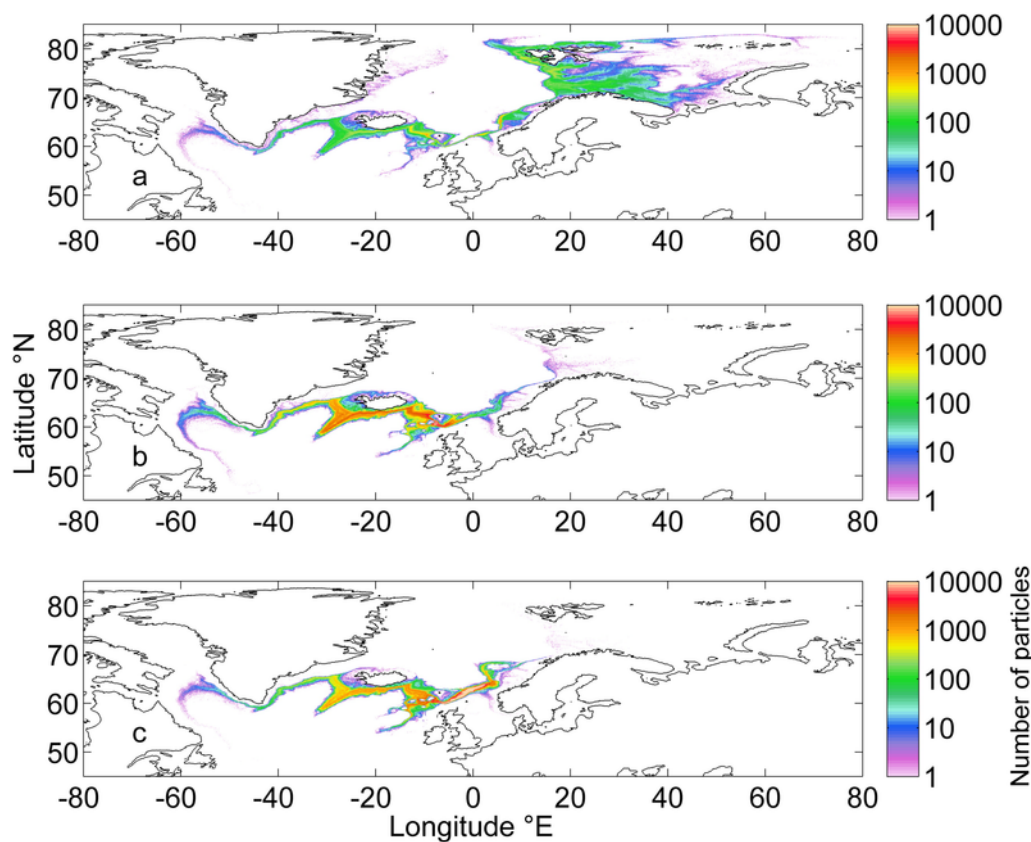


Fig. 8. Particle density plot of particle positions within 200 m of the seabed of all undecayed releases (1994–2009) from: a) 10–450 m; b) 500–950 m; c) 1000–1500 m.

lease location, with some reaching almost as far as the Arctic Ocean, although much less so once decay was considered. Volume transport at the FBC sill has been estimated from instrumental measurements as  $2.1 \pm 0.5$  Sv (Hansen and Osterhus, 2007) which is  $\sim 0.5$  Sv greater than that of the model (1.5 Sv; Marzocchi et al., 2015).

There is evidence of seasonality in volume transport at the FBC (Lake and Lundberg, 2006) and this was also captured here in analysis using particle counts at the sill. Data from the instrumental record have also shown interannual variability in the currents of the FSC (Berk et al., 2013) and the Norwegian Sea (Mork and Skagseth, 2010). Chafik (2012) found that circulation in the FSC may be affected by changes in strength of the North Atlantic Oscillation index (NAO, Walker and Bliss, 1932; Barnston and Livezey, 1987). There was not a clear link between model results here and either monthly or annual NAO values. However, the year in which the maximum distance was travelled by particles (1998) coincided with a strongly negative NAO index.

The biodegradation of hydrocarbons by bacteria is strongly temperature-dependent (Atlas, 1975; Atlas, 1981; Atlas and Hazen, 2011) and temperature was shown to be a factor in the behaviour of microbial communities degrading oil spilled in the 2010 GoM incident (Redmond and Valentine, 2011). Here, temperature-mediated decay of particles, representing the biodegradation of hydrocarbons, affected the oil's spread in the simulations. Particles released in cold, deep water experienced slower decay and persisted for a longer period of time than those released in shallow water, but did not travel as far in slow, deepwater currents. Since results here indicate that oil released in the deep ocean of the FSC may persist for considerably longer than the oil that is present at the surface, the implication is that large areas of the deep ocean would experience prolonged exposure

in the event of a spill. The cold, Arctic influence in the FSC region means that biodegradation rates in deep water there would be relatively slow. This increases the potential for exposure, and therefore the harm done by oil pollution. Although there was evidence that microbial communities in deepwater responded differently to those in surface slicks of the Macondo spill (Redmond and Valentine, 2011), there were also suggestions that biodegradation in the deepwater plumes was limited (Reddy et al. (2011). Recent evidence suggests that biodegradation processes in the deep ocean were impeded by the use of dispersants injected at the Macondo well head (Kleindienst et al., 2015). This further suggests that oil in the colder, more Arctic-influenced FSC might be metabolised particularly slowly and more so if dispersants are used.

Results here indicated that shallow releases of particles were transported the furthest, even after temperature-mediated decay was considered (up to  $\sim 700$  km to the north). Although this implies that a larger area of the shallow ocean would be affected, processes contributing to weathering at and near the surface that were not considered here (e.g. mixing, evaporation, tides) would limit the extent of the oil's travel.

Water-borne hydrocarbons that remained in the deep ocean of the GoM after the Macondo oil well blowout triggered blooms of oil-degrading bacteria (Hazen et al., 2010) and created a higher demand for oxygen in the area of deep water oil plumes (Valentine et al., 2010). Coral communities that were directly beneath the path of the deep hydrocarbon plumes were observed to become stressed, probably resulting from contact with oily sludge that was traced to the Macondo oil (White et al., 2012) and therefore may have resulted from fallout from the midwater oil. The affected coral communities from the GoM provide important evidence that seabed biota are impacted by subsur-

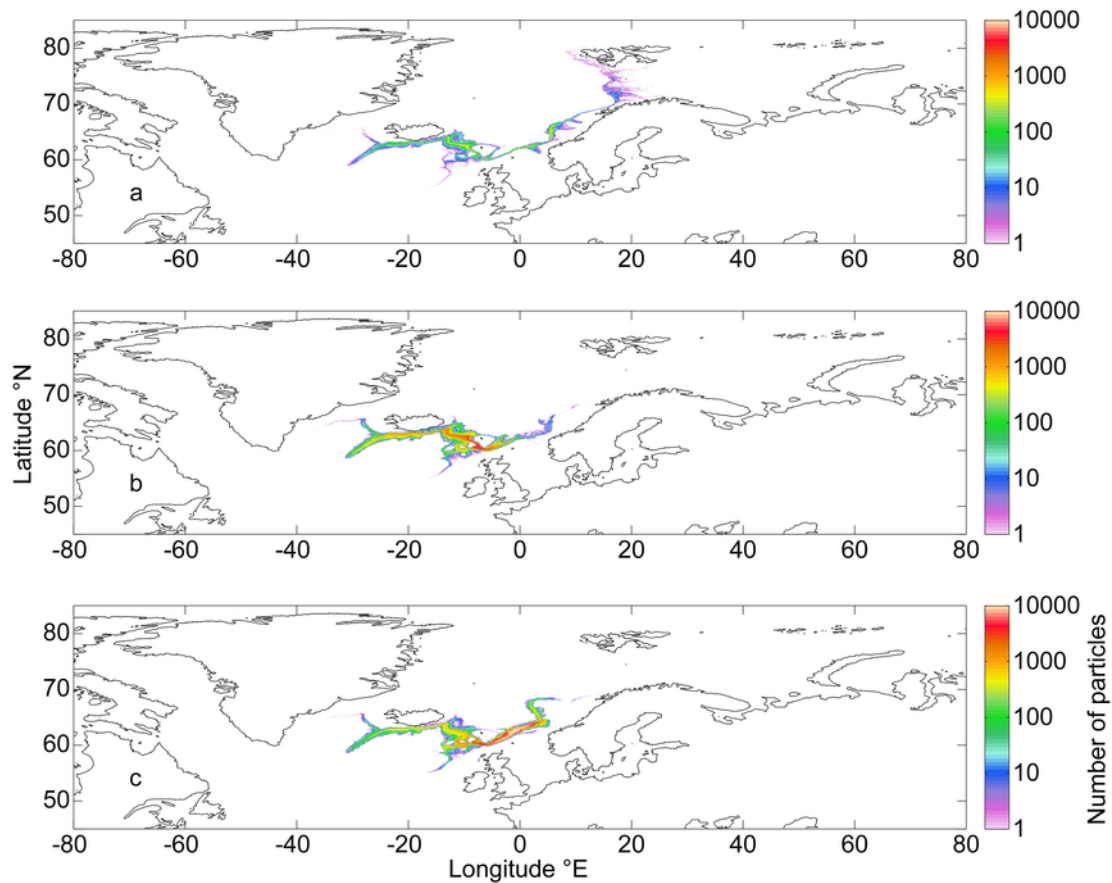


**Fig. 9.** Particle density plot of particle positions within 200 m of the seabed of all decayed releases (1994–2009) from: a) 10–450 m; b) 500–950 m; c) 1000–1500 m. Particle drift was terminated on reaching 10% of initial size.

face oil released from oil well blowouts. It is therefore important to consider the progress of oil on subsurface currents, from which fallout from plumes can clearly occur. There are numerous important benthic features in the coldwater FSC region and beyond, and any future spill could affect unique coldwater coral communities in the region (e.g. the Darwin Mounds Special Area of Conservation, Joint Nature Conservation Committee, c) as well as both pelagic (mackerel and herring) or demersal (cod, haddock) commercial fisheries.

Even once decay was considered, some particles were advected relatively far north towards the Arctic. The ecosystems in the FSC region and further north are influenced by cold waters formed in the Arctic. Species from these cold water environments could be particularly sensitive to oil pollution, as indicated by toxicological studies on Arctic species (Olsen et al., 2007b; Camus et al., 2002, 2003) and experiments have shown that deep water sediments respond to oil contamination with significant increases in sediment community oxygen consumption (Olsen et al., 2007b) and rapid changes in microbial community composition (Main et al., 2015).

We note that there are a number of factors that make direct comparison of the GoM spill with potential spills in the FSC difficult and change the relative risk of drilling in the FSC. There can be great variability in pressure and temperature between wells within both of these regions (UK Government Department of Business, Energy and Industrial Strategy, and Bureau of Ocean Energy Management and United States Geological Survey databases). Therefore the depth of resultant subsurface plumes from an accidental release would depend heavily on the location, conditions, and well depth in addition to the temperature and pressure of oil being released. Since the GoM inci-

dent, there have been a number of technological and operational changes in both well engineering and oil spill response that have been introduced.

The results from this modelling investigation highlight the importance of timing in determining the potential severity of a deep water oil spill. This therefore gives us new insight into the vulnerability of ecosystems in the FSC region, some of which are internationally important, protected areas. Some near-shore physical processes such as wave formation, wave breaking and tides, (all of which would influence transport in shelf seas) are not fully represented in the model so some uncertainty remains with regards to vertical mixing as well as circulation in shallow shelf waters. More work needs to be done to better represent the behaviour of oil after release to reduce uncertainty in its decay rate. Using an ensemble of model runs would reduce the uncertainty in the statistics, and longer runs would enable investigation into the character and mechanisms of interannual variability.

## 5. Conclusions

- 1) In the FSC region, opposing circulation patterns down the water column would strongly affect direction of transport of spilled oil. These model results enable the visualisation of the circulation pathways known from observational studies and hence facilitate the consideration of potential oil spill impacts.
- 2) The timing of a spill in this region could have a critical effect on its severity, based on model results showing interannual variability, and to a certain extent seasonal variability.

**Table 4**

Average percentage of particle days from each release that were within 200 m of seafloor 1994–2001. Values &gt; 50% have been shaded.

Release depth (m)	1994	1995	1996	1997	1998	1999	2000	2001	2002	2003	2004	2005	2006	2007	2008	2009
10	27	20	32	44	31	33	25	19	24	38	40	34	18	26	23	13
50	15	14	33	41	42	27	26	30	35	38	39	29	13	26	32	14
100	8	16	37	40	43	23	19	32	35	36	44	22	10	24	28	19
150	3	14	34	41	44	27	19	35	38	41	48	22	9	23	29	16
200	5	18	32	39	42	26	18	35	38	43	47	17	14	17	26	15
250	9	34	42	41	41	31	29	32	34	46	45	18	20	21	25	17
300	9	38	54	51	38	34	36	23	38	55	48	18	18	27	28	27
350	11	39	53	51	35	26	29	29	39	63	54	13	17	29	28	33
400	14	37	41	40	38	29	36	45	36	65	47	17	21	38	46	42
450	17	35	41	38	51	36	54	74	45	54	41	22	26	47	71	51
500	19	35	51	44	56	45	66	92	53	49	41	27	31	55	86	61
550	19	35	64	52	62	59	74	96	62	41	48	37	36	64	92	72
600	19	37	74	61	67	70	79	98	71	48	52	43	41	70	93	79
650	19	40	83	68	72	76	84	98	77	56	56	46	46	75	93	83
700	16	41	90	76	77	78	87	99	82	71	58	47	47	77	94	85
750	15	42	92	80	79	78	89	99	84	83	62	49	47	78	94	86
800	13	42	94	82	82	79	90	99	86	88	67	51	47	79	93	86
850	8	42	95	85	85	81	90	99	87	90	68	54	47	80	91	86
900	6	43	94	86	87	82	90	99	87	91	70	58	47	82	86	84
950	5	45	94	87	86	81	90	97	87	92	71	59	48	81	84	81
1000	5	47	93	88	84	82	90	95	87	90	68	60	47	82	85	80
1050	5	47	92	86	82	77	89	92	85	90	66	57	47	82	85	77
1100	10	46	90	88	77	74	89	89	84	87	62	49	52	83	84	73
1150	19	43	81	88	73	67	89	85	87	84	60	40	53	83	84	67
1200	31	44	73	88	73	57	88	80	88	82	58	37	55	81	85	62
1250	41	45	67	90	74	48	86	76	93	80	62	39	61	80	86	63
1300	53	49	68	92	79	51	85	78	97	86	65	47	70	81	89	70
1350	67	61	72	94	87	72	86	84	99	90	74	60	77	85	94	78
1400	82	81	87	97	95	88	92	92	99	96	89	74	82	90	99	89
1450	91	89	95	99	98	96	96	98	100	99	97	87	89	95	99	96
1500	98	95	99	100	99	100	100	100	100	100	99	94	96	98	100	99

- 3) The cold, deep water environments of the FSC and Iceland basin are more likely to be heavily impacted than deep waters further north. Conversely, the faster and warmer shallow and surface currents would transport oil furthest north into the Norwegian Sea and towards the Arctic, even with their higher rates of biodegradation.
- 4) Pathways and extent of transport are strongly determined by decay rates of the oil, the depth of establishment of oil plumes and the depths at which they are subsequently maintained.

General circulation models such as NEMO are powerful tools with many potential applications. The surface forcing datasets are realistic (Dussin and Barnier, 2013; Marzocchi et al., 2015) and this reduces uncertainty when applying the model to assess interannual variability. The hindcast output of NEMO is clearly not an operational forecasting tool, but it has been used here to highlight the importance of seasonal and interannual variability of pathways of oil in the deep ocean, and to do so using historically realistic patterns of ocean circulation.

However, there remain large gaps in our understanding of the transport of subsurface oil on ocean currents. Given the continuing expansion of drilling in deeper waters, there is a timely need to understand the full implications of deep water spills in contrasting oceanic regions including the FSC and Arctic Ocean.

#### Uncited references

Joint Nature Conservation Committee, n.d  
 Joint Nature Conservation Committee, n.d

National Oceanic and Atmospheric Administration, n.d

#### Acknowledgements

Support for this work was provided in part by the Natural Environment Research Council (NERC) Marine Environmental Mapping Programme (MAREMAP) and Modelling National Capability. CEM was jointly funded by the SERPENT project ([www.serpentproject.com](http://www.serpentproject.com)) and the University of Southampton.

#### Appendix A. Supplementary data

Supplementary data to this article can be found online at <http://dx.doi.org/10.1016/j.marpolbul.2016.09.041>.

#### References

- Adcroft, A., Hallberg, R., Dunne, J.P., Samuels, B.L., Galt, J.A., Barker, C.H., Payton, D., 2010. Simulations of underwater plumes of dissolved oil in the Gulf of Mexico. *Geophys. Res. Lett.* 37 (18), 1–5.
- Atlas, R.M., 1975. Effects of temperature and crude oil composition on petroleum biodegradation. *Appl. Microbiol.* 30 (3), 396–403.
- Atlas, R.M., 1981. Microbial degradation of petroleum hydrocarbons: an environmental perspective. *Microbiol. Rev.* 45 (1), 180–209.
- Atlas, R.M., Hazen, T.C., 2011. Oil biodegradation and bioremediation: a tale of the two worst spills in U.S. history. *Environ. Sci. Technol.* 45 (16), 6709–6715.
- Barnston, A.G., Livezey, R.E., 1987. Classification, seasonality and persistence of low frequency atmospheric circulation patterns. *Mon. Weather Rev.* 115, 1083–1126.
- Berx, B., Hansen, B., Østerhus, S., Larsen, K.M., Sherwin, T., Jochumsen, K., 2013. Combining in situ measurements and altimetry to estimate volume, heat and salt transport variability through the Faroe–Shetland Channel. *Ocean Sci.* 9 (4), 639–654.
- Bett, B.J., 2001. UK Atlantic margin environmental survey: introduction and overview of bathyal benthic ecology. *Cont. Shelf Res.* 21 (8–10), 917–956.

- Blanke, B., Raynaud, S., 1997. Kinematics of the Pacific equatorial undercurrent: an Eulerian and Lagrangian approach from GCM results. *J. Phys. Oceanogr.* 27, 1038–1053.
- Blanke, B., Arhan, M., Madec, G., Roche, S., 1999. Warm water paths in the equatorial Atlantic as diagnosed with a general circulation model. *J. Phys. Oceanogr.* 29, 2753–2768.
- Brodeau, L., Barnier, B., Treguier, A.-M., Pendu, T., Gulev, S., 2010. An ER-A40-based atmospheric forcing for global ocean circulation models. *Ocean Model* 31 (3–4), 88–104.
- Camilli, R., Reddy, C.M., Yoerger, D.R., Van Mooy, B.A.S., Jakuba, M.V., Kinsey, J.C., McIntyre, C.P., Sylva, S.P., Maloney, J.V., 2010. Tracking hydrocarbon plume transport and biodegradation at Deepwater Horizon. *Science* 330 (6001), 201–204.
- Camus, L., Jones, M.B., Børseth, J.F., Regoli, F., Depledge, M.H., 2002. Heart rate, respiration and total oxyradical scavenging capacity of the Arctic spider crab, *Hyas araneus*, following exposure to polycyclic aromatic compounds via sediment and injection. *Aquat. Toxicol.* 61, 1–13.
- Camus, L., Birkely, S.R., Jones, M.B., Børseth, J.F., Grøsvik, B.E., Gulliksen, B., Lønne, O.J., Regoli, F., Depledge, M.H., 2003. Biomarker responses and PAH uptake in *Mya truncata* following exposure to oil-contaminated sediment in an Arctic fjord (Svalbard). *Sci. Total Environ.* 308 (1–3), 221–234.
- Chafik, L., 2012. The response of the circulation in the Faroe–Shetland Channel to the North Atlantic oscillation. *Tellus* 1, 1–12.
- Dasanayaka, L.K., Yapa, P.D., 2009. Role of plume dynamics phase in a Deepwater oil and gas release model. *J. Hydro Environ. Res.* 2 (4), 243–253.
- Dussin, R., Barnier, B., 2013. The Making of DFS 5.1. DRAKKAR Collaboration (39 pp.).
- Hansen, B., Osterhus, S., 2007. Faroe Bank Channel overflow 1995–2005. *Prog. Oceanogr.* 75, 817–856.
- Hazen, T.C., Dubinsky, E.A., Desantis, T.Z., Andersen, G.L., Piceno, Y.M., Singh, N., Jansson, J.K., Probst, A., Borglin, S.E., Fortney, J.L., Stringfellow, W.T., Bill, M., Conrad, M.E., Tom, L.M., Chavarria, K.L., Alusi, T.R., Lamendella, R., Joyner, D.C., Spier, C., Baelum, J., Auer, M., Zemla, M.L., Chakraborty, R., Sonnenthal, E.L., D'haeseleer, P., Holman, H.N., Osman, S., Lu, Z., Van Nostrand, J.D., Deng, Y., Zhou, J., Mason, O.U., 2010. Deep-sea oil plume enriches indigenous oil-degrading bacteria. *Science* 330, 204–208.
- Johansen, , 2003. Development and verification of deep-water blowout models. *Mar. Pollut. Bull.* 47 (9–12), 360–368.
- Johansen, , Rye, H., Cooper, C., 2003. DeepSpill – field study of a simulated oil and gas blowout in deep water. *Spill Sci. Technol. Bull.* 8 (5–6), 433–443.
- Joint Nature Conservation Committee, a. North-east Faroe–Shetland Channel nature conservation marine protected area (NCOMPA). In: <http://jncc.defra.gov.uk/page-6483> (Accessed 07/03/2016).
- Joint Nature Conservation Committee, b. Faroe–Shetland Sponge Belt (NCOMPA). In: <http://jncc.defra.gov.uk/page-6479> Accessed 07/03/2016.
- , s. In: <http://jncc.defra.gov.uk/page-6491>.
- J, a c and site of community i. In: <http://jncc.defra.gov.uk/page-6545>.
- Joint Nature Conservation Committee, c. Darwin mounds cSAC/SCI. In: <http://jncc.defra.gov.uk/page-6531> (Accessed 07/03/2016).
- Jones, D.O.B., Bett, B.J., Tyler, P.A., 2007. Megabenthic ecology of the Faroe–Shetland Channel: a photographic study. *Deep-Sea Res. I Oceanogr. Res. Pap.* 54, 1111–1128.
- Jutzeler, M., Marsh, R., Carey, R.J., White, J.D.L., Talling, P.J., Karlstrom, L., 2014. On the fate of pumice rafts formed during the 2012 Havre submarine eruption. *Nat. Commun.* 5, 3660.
- Kessler, J.D., Valentine, D.L., Redmond, M.C., Du, M., Chan, E.W., Mendes, S.D., Quiroz, E.W., Villanueva, C.J., Shusta, S.S., Werra, L.M., Yvon-Lewis, S.A., Weber, T.C., 2011. A persistent oxygen anomaly reveals the fate of spilled methane in the deep Gulf of Mexico. *Science* 331 (6015), 312–315.
- Kleindienst, S., Seidel, M., Ziervogel, K., Grim, S., Loftisa, K., Harrison, S., Malkina, S.Y., Perkins, M.J., Field, J., Soginc, M.L., Dittmare, T., Passow, U., Medeirosa, P.M., Joye, S.B., 2015. Chemical dispersants can suppress the activity of natural oil-degrading microorganisms. *Proc. Natl. Acad. Sci.* 12 (48), 14900–14905.
- Lake, I., Lundberg, P., 2006. Seasonal barotropic modulation of the deep-water overflow through the Faroe Bank Channel. *J. Phys. Oceanogr.* 36, 2328–2339.
- Leffer, W.L., Pattarozzi, R., Sterling, G., 2011. Deepwater Petroleum Exploration & Production a Nontechnical Guide, 2nd edition Penwell (351 pp.).
- Lindo-Atichati, D., Paris, C.B., Le Hénaff, M., Schedler, M., Valladares Juárez, A.G., Müller, R., 2014. Simulating the effects of droplet size, high-pressure biodegradation, and variable flow rate on the subsea evolution of deep plumes from the Macondo blowout. *Deep-Sea Res. II Top. Stud. Oceanogr.* <http://dx.doi.org/10.1016/j.dsr2.2014.01.011>.
- Liu, Y., Weisberg, R.H., Hu, C., Zheng, L., 2011. Tracking the Deepwater horizon oil spill: a modeling perspective. *Ocean Model* 92 (6), 2010–2012.
- Liu, Y., Weisberg, R.H., Hu, C., Zheng, L., 2011. Trajectory forecast as a rapid response to the Deepwater horizon oil spill. *Geophys. Monogr. Ser.* 195, 153–165.
- Lohmann, K., Jungclaus, J.H., Matei, D., Mignot, J., Menary, M., Langehaug, H.R., Ba, J., Gao, Y., Ottera, O.H., Park, W., Lorenz, S., 2014. The role of subpolar deep water formation and Nordic seas overflows in simulated multidecadal variability of the Atlantic meridional overturning circulation. *Ocean Sci.* 10 (2), 227–241.
- Madec, G., 2008. NEMO Ocean Engine. (2011 pp.).
- Main, C.E., Ruhl, H.A., Jones, D.O.B., Yool, A., Thornton, B., Mayor, D.M., 2015. Hydrocarbon contamination affects deep-sea benthic oxygen uptake and microbial community composition. *Deep Sea Res. I* 100, 79–87.
- Mariano, A.J., Kourafalou, V.H., Srinivasan, A., Kang, H., Halliwell, G.R., Ryan, E.H., Roffer, M., 2011. On the modeling of the 2010 Gulf of Mexico oil spill. *Dyn. Atmos. Oceans* 52 (1–2), 322–340.
- Marzocchi, A., Hirschi, J.J.-M., Holliday, N.P., Cunningham, S.A., Blaker, A.T., Coward, A.C., 2015. The North Atlantic subpolar circulation in an eddy-resolving global ocean model. *J. Mar. Syst.* 142, 126–143.
- McNutt, M., Camilli, R., Guthrie, G., Hsieh, P., Labson, V., Lehr, B., Maclay, D., Ratzel, A., Sogge, M., 2011. Assessment of Flow Rate Estimates for the Deepwater Horizon/Macondo well Oil Spill. In: Flow Rate Technical Group Report to the National Incident Command. Interagency Solutions Group (March 10, 2011. 30 pp.).
- Montagna, P.A., Baguley, J.G., Cooksey, C., Hartwell, I., Hyde, L.J., Hyland, J.L., Kalke, R.D., Kracker, L.M., Reuscher, M., Rhodes, A.C.E., 2013. Deep-sea benthic footprint of the Deepwater horizon blowout. *PLoS One* 8 (8), e70540.
- Mork, K.A., Skagseth, , 2010. A quantitative description of the Norwegian Atlantic current by combining altimetry and hydrography. *Ocean Sci.* 6 (4), 901–911.
- , In: National Research Council, 2005. Dispersant-Oil Interactions and Effectiveness Testing. In: Oil spill dispersants: efficacy and effects. National Academies Press (395 pp.).
- Olsen, G. H., Sva, E., Carroll, J., Camus, L., De Coen, W., Smolders, R., Overaas, H., & Hylland, K. (2007). Alterations in the energy budget of Arctic benthic species exposed to oil-related compounds. *Aquatic Toxicology*, 83(2), 85–92., G.H., S.E., J., Cam L., W., R., , G.H., E., J., L., W., R., H. K. . *Aquat. Toxicol.* ( ), – (2007).
- Paris, C.B., Le, M., Aman, Z.M., Subramaniam, A., Helgers, J., Wang, D., Kourafalou, V.H., Srinivasan, A., 2012. Evolution of the Macondo well blowout: simulating the effects of the circulation and synthetic dispersants on the subsea oil transport. *Environ. Sci. Technol.* 46, 13293–13302.
- Paris, C.B., Helgers, J., van Sebille, E., Srinivasan, A., 2013. Connectivity modeling system: a probabilistic modeling tool for the multi-scale tracking of biotic and abiotic variability in the ocean. *Environ. Model. Softw.* 42, 47–54.
- Putman, N.F., Scott, R., Verley, P., Marsh, R., Hays, G.C., 2012. Natal site and off-shore swimming influence fitness and long-distance ocean transport in young sea turtles. *Mar. Biol.* 159 (10), 2117–2126.
- Reddy, C.M., Arey, J.S., Seewald, J.S., Sylva, S.P., Lemkau, K.L., Nelson, R.K., Carmichael, C.A., MacIntyre, C.P., Fenwick, J., Ventura, G.T., Van Mooy, B.A.S., Camilli, R., 2011. Composition and fate of gas and oil released to the water column during the Deepwater horizon oil spill. *Proc. Natl. Acad. Sci.* 109 (50), 20229–20234.
- Redmond, M.C., Valentine, D.L., 2011. Natural gas and temperature structured a microbial community response to the Deepwater horizon oil spill. *Proc. Natl. Acad. Sci.* 109 (50), 20292–20297.
- Rossby, T., Prater, M.D., Sjøland, H., 2009. Pathways of inflow and dispersion of warm waters in the Nordic seas. *J. Geophys. Res.* 114 (C4), , C04011.
- Ryerson, T.B., Camilli, R., Kessler, J.D., Kujawinski, E.B., Reddy, C.M., Valentine, D.L., Atlas, E., Blake, D.R., de Gou, J., Meinardi, S., Parrish, D.D., Peischl, J., Seewald, J.S., Warneke, C., 2012. Chemical data quantify Deepwater horizon hydrocarbon flow rate and environmental distribution. *Proc. Natl. Acad. Sci.* 109 (50), 20246–20253.
- Sherwin, T.J., Turrell, W.R., 2005. Mixing and advection of a cold water cascade over the Wyville Thomson ridge. *Deep-Sea Res. I Oceanogr. Res. Pap.* 52 (8), 1392–1413.
- Sherwin, T.J., Williams, M.O., Turrell, W.R., Hughes, S.L., Miller, P.I., 2006. A description and analysis of mesoscale variability in the Färoe-Shetland Channel. *J. Geophys. Res.* 111 (C3), C03003.
- Smallwood, J.R., Kirk, W.J., 2005. Paleocene Exploration in the Faroe – Shetland Channel: Disappointments and Discoveries. In: Dore, A.G., Vining, B.A. (Eds.), *Petroleum Geology: North-West Europe and Global Perspectives—Proceedings of the 6th Petroleum Geology Conference*.
- Socolofsky, S.A., Adams, E.E., Sherwood, C.R., 2011. Formation dynamics of subsurface hydrocarbon intrusions following the Deepwater horizon blowout. *Geophys. Res. Lett.* 38 (9), 2–7.
- Turrell, W.R., Slessor, G., Adams, R.D., Payne, R., Gillibrand, P.A., 1999. Decadal variability in the composition of Faroe Shetland Channel bottom water. *Deep-Sea Res. I Oceanogr. Res. Pap.* 46 (1), 1–25.
- Valentine, D.L., Kessler, J.D., Redmond, M.C., Mendes, S.D., Heintz, M.B., Farwell, C., Hu, L., Kinnaman, F.S., Yvon-Lewis, S., Mengran, D., Chan, E.W., Garcia Tigreros, F., Villanueva, C.J., 2010. Propane respiration jump-starts microbial response to a deep oil spill. *Science* 330, 208–211.

- Valentine, D.L., Mezić, I., Macesic, S., Crnjarić-Zić, N., Ivic, S., Hogan, P.J., Fonoberov, V.A., Loire, S., 2012. Dynamic Autoinoculation and the Microbial Ecology of a Deep Water Hydrocarbon Irruption. *Proc. Natl. Acad. Sci.* 1–6.
- Valentine, D.L., Fisher, G.B., Bagby, S.C., Nelson, R.K., Reddy, C.M., Sylva, S.P., Woo, M.A., 2014. Fallout plume of submerged oil from. *Deepwater Horiz. Proc. Natl. Acad. Sci.* 111 (45), 15906–15911.
- Walker, G.T., Bliss, E.W., 1932. World weather V. *Mem. R. Meteorol. Soc.* 4, 53–84.
- White, H.K., Hsing, P.-Y., Cho, W., Shank, T.M., Cordes, E.E., Quattrini, A.M., Nelson, R.K., Camilli, R., Demopolous, A.W.J., German, C.R., Brooks, J.M., Roberts, H.H., Shedd, W., Reddy, C.M., Fisher, C.R., 2012. Impact of the Deepwater horizon oil spill on a deep-water coral community in the Gulf of Mexico. *Proc. Natl. Acad. Sci.* 109 (50), 20303–20308.
- Yapa, P.D., Dasanayaka, L.K., Bandara, U.C., Nakata, K., 2008. Modeling the impact of an accidental release of methane Gas in Deepwater. *Oceans 2008*, 1–10 (15–18 Sept 2008).

UNCORRECTED PROOF